THE JOURNAL OF PHYSICAL CHEMISTRY Letters

pubs.acs.org/JPCL Letter

Nonthermalized Precursor-Mediated Dissociative Chemisorption at High Catalysis Temperatures

Raquel Moiraghi, Ariel Lozano, Eric Peterson, Arthur Utz, Wei Dong,* and H. Fabio Busnengo*

Cite This: J. Phys. Chem. Lett. 2020, 11, 2211−2218 Read Online

ACCESS | Metrics & More | Article Recommendations | Supporting Information

ABSTRACT: Quasiclassical trajectory calculations and vibrational-state-selected beam-surface measurements of CH_4 chemisorption on Ir(111) reveal a nonthermal, hot-molecule mechanism for C−H bond activation. Low-energy vibrationally excited molecules become trapped in the physisorption well and react before vibrational and translational energies accommodate the surface. The reaction probability is strongly surface-temperature-dependent and arises from the pivotal role of Ir atom thermal motion. In reactive trajectories, the mean outward Ir atom displacement largely exceeds that of the transition-state geometry obtained through a full geometry optimization. The study also highlights a new way for (temporary) surface defects to impact high-temperature heterogeneous catalytic reactivity. Instead of reactants diffusing to and competing for geometrically localized lower barrier sites, transient, thermally activated surface atom displacements deliver low-barrier surface reaction geometries to the physisorbed reactants.

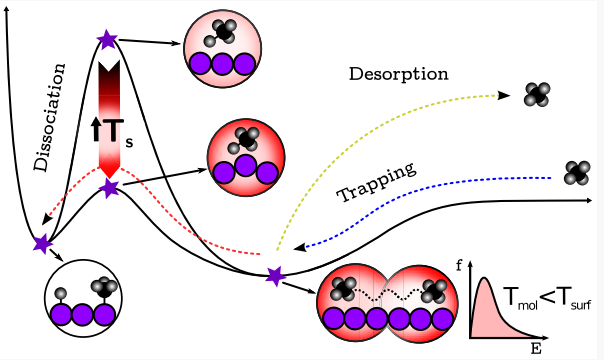

Because among the many elementary steps involved in a chemical reaction on a solid surface, dissociative adsorption is very often the rate-limiting one, "bond-breaking upon chemisorption is perhaps the most important role of a catalyst".[1] This is the case, in particular, for the heterogeneous catalytic steam reforming of natural gas used in industry to produce molecular hydrogen, which is rate-limited by the first C−H bond-breaking of methane and proceeds at high temperatures of ∼1000−1300 K.[2] This has motivated a large number of well-controlled surface science experiments using supersonic molecular beams (SMB) that have investigated the effect of the surface temperature, T_s, and the methane molecule's translational energy, E_i, and vibrational state on the initial reactive sticking probability, S_0. (See, for example, refs 3−7 and references therein.) The main common signature observed for many transition-metal surfaces is an abrupt increase (up to five orders of magnitude) in S_0 with increasing E_i (i.e., $\partial S_0/\partial E_i > 0$, see, e.g., figure 29 of ref 4) simply due to the growing number of accessible dissociation pathways. Nevertheless, on Ir(111),[3,7] Ir(110),[8] and Pt(110),[9,10] methane molecules at low impact energies ($E_i \lesssim 0.1$ eV) show an initial decrease in the $S_0(E_i)$ curve (i.e., $\partial S_0/\partial E_i < 0$) that is considered to be a fingerprint for a precursor-mediated (or trapping-mediated) chemisorption mechanism.

In a precursor-mediated mechanism, the approaching molecule first dissipates enough of its incident kinetic energy to become a resident in a transient precursor state in a potential-energy well resulting from the interplay of long-range attractive and short-range repulsive interactions between the adsorbate and the substrate. The depth and location of such a well certainly depends on the nature of the molecule−surface interaction (here we focus only on the so-called intrinsic precursors that do not involve the presence of preadsorbed species[11]), but, in general, trapping-mediated dissociation is more efficient for low translational energy molecules whose modest E_i is most easily transferred to other degrees of freedom (DOF) or dissipated in a single molecule−surface collision. Trapping allows the molecules to remain near the surface for a longer time and have an increased chance of finding a favorable pathway for dissociative chemisorption.[12] As E_i increases, trapping-mediated dissociation drops roughly exponentially due to the sharply decreasing probability of trapping into the precursor state, P_{trapp}. At higher E_i, direct dissociation prevails. In between these two regimes (∼0.1 eV for CH_4/Ir(111)[3,7]), both mechanisms contribute significantly to the observed E_i and T_s dependence of S_0, which is the sum of precursor-mediated and direct dissociation probabilities ($S_0 = S_{dir} + S_{trapp}$). This explains the nonmonotonic shape of the $S_0(E_i)$ curve. Other molecule−surface systems also exhibit a low-E_i precursor-mediated channel, for example, H_2 on various

Received: January 26, 2020
Accepted: February 19, 2020
Published: February 19, 2020

https://dx.doi.org/10.1021/acs.jpclett.0c00260
J. Phys. Chem. Lett. 2020, 11, 2211−2218

surfaces of Pd,[13] Ni,[14] W,[15] and Pt,[16] N_2/W(100),[17−19] O_2/Pt(111),[20] and ethane/Ir(110),[21] but in all of these cases, the precursor-mediated reactivity is most pronounced at low surface temperatures and ceases when T_s increases ($\partial S_0/\partial T_s < 0$). In contrast, the precursor-mediated reactivity of CH_4/Ir(111) increases with increasing T_s up to 1000 K ($\partial S_0/\partial T_s > 0$)[3] despite the expected short surface residence lifetime for the weakly bound precursor.[22] The differing manifestations of this reaction channel and its potential importance in high-temperature industrial catalysis, in which a majority of molecules contain chemically significant internal vibrational energy but modest E_i ideal for trapping, motivate our work.

The long-standing wisdom about precursor-mediated chemisorption and, in particular, its T_s dependence, supposes that after a molecule is trapped, it thermally equilibrates in the precursor state. Then, the dissociation probability is determined by the competition between the thermal rate constants for chemisorption (k_c) and desorption (k_d): $k_{d,c} = \nu_{d,c} \exp[-E_{d,c}/(k_B T_s)]$, where k_B is the Boltzmann constant and E_d (E_c) and ν_d (ν_c) are the corresponding energy barriers and pre-exponential factors for desorption (chemisorption), respectively. However, vibrational state-resolved measurements of methane in its ground vibrational state ($\nu = 0$) and $\nu_3 = 1$ C−H stretching states undermine this assumption. They show that S_0 for $CH_4(\nu_3 = 1)$, is significantly greater than that for $CH_4(\nu = 0)$, so the full thermalization of vibrational states does not occur in the precursor state.[7] The authors cite the kinetic competition between the surface residence time of physisorbed CH_4 molecules[23] and the vibrational energy dynamics to argue that molecules most likely desorb before significant vibrational energy redistribution or quenching occurs on the surface.[24] Others have raised questions about the role of weakly bound precursor states for methane at high real catalysis temperatures,[22] and recent studies of $CO(\nu = 2)$ scattering from Au(111) provide further evidence of a slower than expected vibrational relaxation of physisorbed molecules on surfaces.[25−27]

The complicated interplay between direct and precursor-mediated mechanisms and the lack of a priori justification for the use of thermal rate constants motivate our use of dynamical simulations to study the low-E_i reactivity of methane on a catalytically active transition-metal surface. The goal is to disentangle experimentally observed reactivity patterns and reveal the role and mechanism of direct and precursor-mediated chemisorption for the most relevant values of E_i and T_s under real-catalysis conditions. Performing calculations that account for the coupled time evolution of both molecular and surface degrees of freedom presents formidable technical challenges and guides our choice of method. Integration times of tens of picoseconds (the mean lifetime of the precursor state[23]) are required with a time resolution of a tenth of a femtosecond to properly describe the fast methane vibrations, resulting in up to $\sim 10^6$ time steps per trajectory. Acceptable statistical errors for the calculation of S_0 values as small as $\sim 10^{-4}$ can require up to $\sim 10^{+5}$ trajectories per impact condition. The necessary computational effort for an *ab initio* molecular dynamics calculation[28] would be about four to five orders of magnitude beyond the currently attainable limit.

In this work, we overcome this limitation through quasiclassical trajectory (QCT) calculations that make use of a highly accurate Tersoff-like[29] reactive force field (RFF) constructed from a large set of density functional theory (DFT) data.[30,31] The DFT calculations made use of the semilocal Perdew−Burke−Ernzerhof (PBE) functional[32] for electronic exchange and correlation, and we have added a long-distance van der Waals empirical correction to the RFF to properly account for methane physisorption. Details of the RFF parametrization and its performance and the DFT and QCT calculations are provided in the Supporting Information. Our RFF-based approach allows us to treat the DOF of both molecular and metal atoms on an equal footing. Its relatively low computational cost makes it possible to integrate a large number of trajectories to obtain statistically converged results, even in the present case of low sticking probabilities and long adsorbate−substrate interaction times. We report dissociative adsorption probabilities of CH_4 in its ground vibrational state $CH_4(\nu = 0)$, and in the excited antisymmetric C−H stretching state $CH_4(\nu_3 = 1)$ on Ir(111) at high surface temperatures close to those of real catalysis. The calculated results are compared with previously published state-resolved measurements of S_0 at T_s = 1000 K,[7] conventional beam surface measurements S_0,[3] and previously unpublished state-resolved measurements performed at a range of E_i and T_s values as low as 600 K. For these new measurements, a supersonic molecular beam of methane impinged on a clean Ir(111) surface was held at the desired T_s. The molecular beam source was held at or slightly above room temperature for all of the measurements, and seeding techniques were used to vary the incident kinetic energy of the methane molecules. Under these conditions, very few thermally excited vibrational states were present in the beam, and vibrational ground-state molecules, $\nu = 0$, dominated the measured S_0. The reactivity of the $\nu_3 = 1$ state was measured using a narrow-line-width infrared laser to selectively excite a significant fraction of $\nu = 0$ molecules in the beam to the $\nu_3 = 1$, $J = 2$ vibrational and rotational level. A comparison of the measured reactivity with and without laser excitation yielded the state-resolved values of S_0 for $CH_4(\nu_3 = 1)$ presented here. Reference 7 details the relevant experimental methods and data analysis procedures. Our QCT calculations give results in excellent agreement with experiments and allow us to shed new light on the way that precursor-mediated chemisorption takes place for CH_4/Ir(111) and its influence on the E_i and T_s dependence of S_0 at high surface temperatures close to those of real steam reforming catalysis.

In Figure 1, we compare QCT results for S_0 of $CH_4(\nu = 0)$ and $CH_4(\nu_3 = 1)$ on Ir(111) with available experimental data.[3,7] Our simulations provide results in very good agreement with experiments in many respects. For T_s = 1000 K (Figure 1a), they reproduce well the strong increase in S_0 with increasing E_i above ~0.10 eV (in what follows, referred to as the high-energy regime) and also its decrease ($\partial S_0/\partial E_i < 0$) at lower energies (the low-energy regime). Thus our results properly account for the existence of two distinct dissociation mechanisms: one favored by small and the other by large impact energies for both $CH_4(\nu = 0)$ and $CH_4(\nu_3 = 1)$. Our QCT calculations also predict values of S_0 for $CH_4(\nu_3 = 1)$ that are significantly higher than those for $CH_4(\nu = 0)$ in both the low- and high-energy regimes in very good agreement with experiments, although for $E_i \gtrsim 0.1$ eV, the theoretical vibrational efficacy, η_{vib}, is somewhat smaller than the experimental one: η_{vib} = 90/360 meV = 0.25 vs 0.42.[7] A slight overestimation of experimental sticking probabilities for ground-state molecules and good agreement for vibrationally pre-excited ones have also been found in a similar DFT−PBE-based QCT description of CH_4/Pt(111).[31,33] QCT results can

https://dx.doi.org/10.1021/acs.jpclett.0c00260
J. Phys. Chem. Lett. 2020, 11, 2211−2218

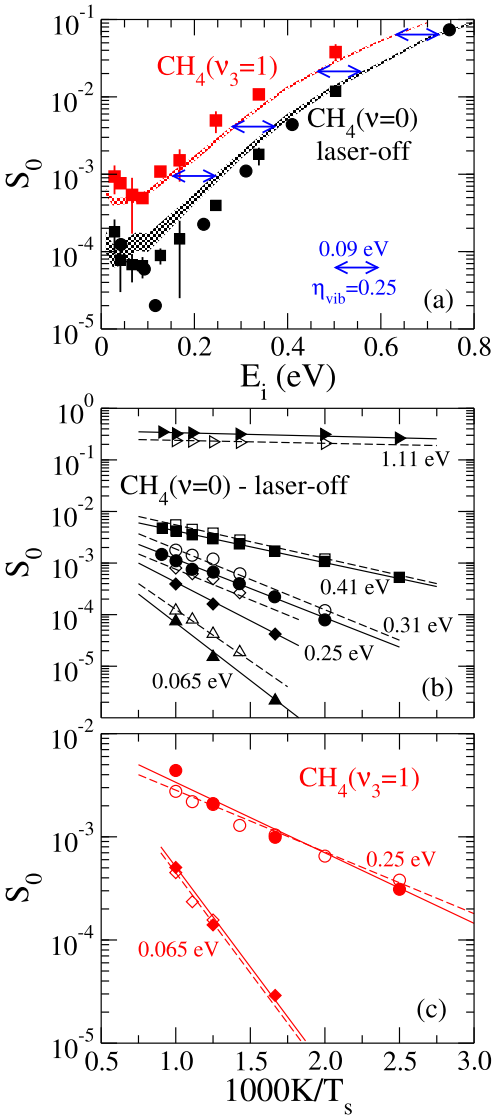

Figure 1. (a) $S_0(E_i)$ for initially nonrotating $CH_4(\nu = 0)$ (black) and $CH_4(\nu_3 = 1)$ (red) at normal incidence for T_s = 1000 K. The shaded areas account for statistical errors of theoretical results (present work): $\Delta S_0 = (S_0 \times (1 - S_0)/N_{trajs})^{1/2}$, where N_{trajs} is the number of computed trajectories. The symbols represent experimental data: ●,[3] ■.[7] (b) Arrhenius plot: S_0 as a function of 1000 K/T_s for $CH_4(\nu = 0)$ (theory, open symbols (present work)) and under laser-off conditions (experiments, filled symbols[3]) at normal incidence. ▶, E_i = 1.11 eV; ■: E_i = 0.41 eV; ●: E_i = 0.31 eV; ◆: E_i = 0.25 eV; ▲: E_i = 0.065 eV. (c) Same as panel b but for $CH_4(\nu_3 = 1)$ (theory and experiments (present work)): ●, E_i = 0.25 eV; ◆, E_i = 0.065 eV.

be affected by artificial intramolecular vibrational redistribution (IVR).[28] Part of the energy initially deposited in the ν_3 antisymmetric stretching mode might flow to other vibrational modes, in particular, those with a similar frequency like the ν_1 symmetric stretching mode. However, the good agreement with experiments obtained here for $CH_4(\nu_3 = 1)$ suggests that IVR is small or S_0 is not very sensitive to this IVR, probably due to a moderate mode selectivity. Further clarification of this issue certainly deserves further investigation. The T_s effects observed experimentally are also very well reproduced for both $CH_4(\nu = 0)$ (Figure 1b) and $CH_4(\nu_3 = 1)$ (Figure 1c): S_0 increases moderately with increasing T_s for $E_i \simeq 1$ eV and much more significantly at lower E_i. Theory and experiment both have $\partial S_0/\partial T_s > 0$, irrespective of the initial molecular impact energy. Thus the dominant dissociation mechanisms in the high- and low-energy regimes are both affected by T_s in qualitatively the same way, although quantitatively much more strongly at low impact energies. The very good overall agreement with experiments makes us confident about the validity of our theoretical approach for investigating in more detail precursor-mediated chemisorption and its interplay with the direct mechanism. Because the E_i and T_s dependences of S_0 for $CH_4(\nu = 0)$ and $CH_4(\nu_3 = 1)$ are basically the same, we focus our analysis on the case of $CH_4(\nu_3 = 1)$, for which statistical errors can be reduced more easily due to the higher sticking probabilities.

To quantify the role of the precursor-mediated and direct mechanisms, we have associated all of the trajectories where the molecule remains close to the Ir(111) surface after more than four rebounds with trapping (i.e., $N_{reb} \geq 5$). We call N^c_{trapp} (N^d_{trapp}) the number of molecules that chemisorb (desorb) after being temporarily trapped and N^c_{dir} (N^d_{dir}) the number of those that chemisorb (are scattered back to vacuum) directly, that is, with $N_{reb} < 5$. Hence, the total number of chemisorbed (unreactive) trajectories is $N^c = N^c_{trapp} + N^c_{dir}$ ($N^d = N^d_{trapp} + N^d_{dir}$); the trapping-mediated (direct) chemisorption probability is $S_{trapp} = N^c_{trapp}/N_{traj}$ ($S_{dir} = N^c_{dir}/N_{traj}$), and the trapping probability is $P_{trapp} = (N^c_{trapp} + N^d_{trapp})/N_{traj}$, where N_{traj} is the total number of integrated trajectories.

The values of S_{trapp}, S_{dir}, and $S_0 = S_{trapp} + S_{dir}$ obtained for $CH_4(\nu_3 = 1)$/Ir(111) at T_s = 1000 K are shown in Figure 2a. They show that the initial decrease in S_0 is due to the E_i dependence of S_{trapp} that decreases exponentially when E_i increases (e.g., by a factor of ~50, from 0.01 to 0.20 eV). In contrast, $\partial S_{dir}/\partial E_i > 0$ over the entire range of impact energies considered. This E_i dependence dominates S_0 for $E_i \gtrsim 0.1$ eV, for which the direct dissociation mechanism dominates. Interestingly, the trapping-mediated pathway and the non-monotonic behavior of S_0 for $CH_4(\nu_3 = 1)$/Ir(111) are completely lost at T_s= 1000 K if we remove the van der Waals correction from our RFF (dashed line in Figure 2a). (In Figure 2a, S_0 (NO vdW) is smaller than S_{dir} because removing the van der Waals corrections results in the reflection of low-energy molecules back into the vacuum far from the surface.) Thus trapping-mediated is observed in the simulations only when long-distance van der Waals interactions are taken into account. The definite proof that molecules are trapped in the physisorption well is provided by Figure 2b. It shows that the distribution of the molecular heights above the surface recorded at interaction time t = 5 ps (red area) is entirely restricted to the region of the physisorption well of the RFF.

We have examined the dependence of P_{trapp} on E_i, T_s, and the methane vibrational state. When T_s = 1000 K, $P_{trapp} \approx 0.7$ in the limit $E_i \rightarrow 0$, and it decreases exponentially as E_i increases (Figure 2a). Very similar results are obtained for lower temperatures because P_{trapp} barely depends on T_s (Figure 2c). In this respect, our results are consistent with the experimental data of Mullins and coworkers[3] and agree well with the results of molecular dynamics simulations based on an empirical unreactive molecule−surface potential.[23] Finally, it is worth mentioning that the values of P_{trapp} do not depend on the initial vibrational state of the molecules, which is in line with experiments performed by Beck and coworkers for methane on Pt(111).[34] The superposition of P_{trapp} and $S_{trapp} \times const$ (*const* = 1520) in Figure 2a clearly shows that the E_i

https://dx.doi.org/10.1021/acs.jpclett.0c00260
J. Phys. Chem. Lett. 2020, 11, 2211−2218

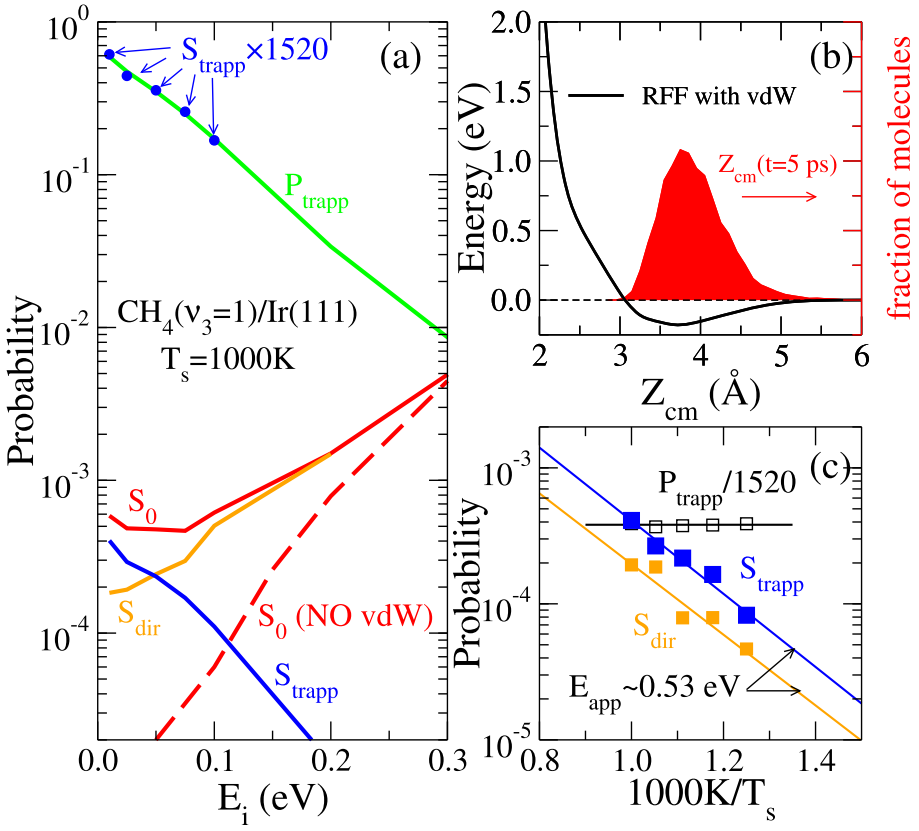

Figure 2. (a) S_0 (red), S_{dir} (orange), S_{trapp} (blue), and P_{trapp} (green) for $CH_4(\nu_3 = 1)$/Ir(111) at T_s = 1000 K. Dashed red line: S_0 obtained without including van der Waals corrections into the RFF. Blue ●: $S_0 \times 1520$ depicted to help the comparison with P_{trapp}. (b) CH_4/Ir(111) interaction potential at a long distance from the surface with the van der Waals correction and the Z_{cm} distribution of trapped molecules at time t = 5 ps (red area) for $CH_4(\nu_3 = 1)$, E_i = 0.01 eV, and T_s = 1000 K. (c) Arrhenius plot for $S_{trapp} \approx 0.19 \times \exp(-0.53\ \text{eV}/k_B T_s)$ (blue), $S_{dir} \approx 0.10 \times \exp(-0.53\ \text{eV}/k_B T_s)$ (orange), and $P_{trapp}/1520$ (black) for $CH_4(\nu_3 = 1)$/Ir(111) (E_i = 0.01 eV).

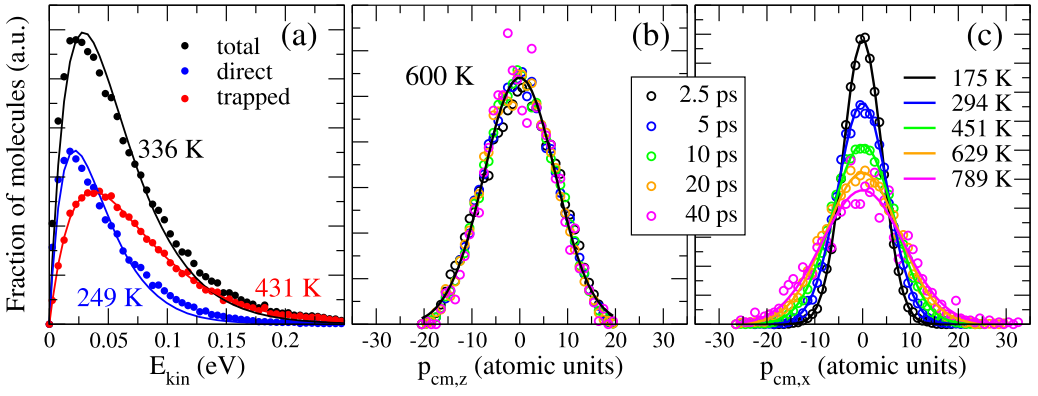

Figure 3. (a) Translational kinetic energy distribution of $CH_4(\nu_3 = 1)$ molecules scattered back to vacuum from Ir(111) at T_s = 1000 K. (b) Distribution of translational linear momentum perpendicular to the surface of $CH_4(\nu_3 = 1)$ molecules trapped near Ir(111) for different interaction times at T_s = 1000 K. (c) Panel b but for a momentum directed parallel to the surface.

dependence of S_{trapp} comes from the P_{trapp} dependence on E_i. Thus $S_{trapp}(E_i, \nu, T_s)$ can be factorized as follows

$$S_{trapp}(E_i, \nu, T_s) = P_{trapp}(E_i) \times \alpha(\nu, T_s) \quad (1)$$

where $\alpha(\nu, T_s)$ is the fraction of trapped molecules that dissociatively chemisorb, which depends on the initial molecular vibrational state (denoted by ν) and T_s but not on E_i. Because α does not depend on E_i, our results show that after only five rebounds, trapped molecules lose memory of their initial translational kinetic energy. Nevertheless, this memory loss does not imply that molecules are translationally thermalized on the surface after only five rebounds, as will be shown later.

Figure 2c shows Arrhenius plots for S_{trapp} and S_{dir} for $CH_4(\nu_3 = 1)$ with E_i = 0.01 eV. Both S_{trapp} and S_{dir} increase with surface temperature and present an Arrhenius-like T_s dependence with apparent activation energies, E_{app}, that are very similar (~0.53 eV). This is surprising because of the significantly different characteristic interaction times involved in both mechanisms (a fraction vs tens of picoseconds) and suggests a similar origin of the T_s effect in both cases. The usual way to rationalize the T_s

https://dx.doi.org/10.1021/acs.jpclett.0c00260
J. Phys. Chem. Lett. 2020, 11, 2211−2218

dependence of S_{trapp} (or similarly, that of the coefficient α) is to assume that trapped molecules thermalize on the surface. Then, α results from the competition between thermal rate constants of chemisorption and desorption from the physisorption well

$$\alpha(\nu, T_s) = \frac{k_c}{k_c + k_d} = \frac{1}{1 + \nu_d/\nu_c \exp[-(E_d - E_c)/k_B T_s]} \quad (2)$$

Nonetheless, our QCT calculations unambiguously show that molecules temporarily trapped in the physisorption well never reach thermalization on Ir(111) at 1000 K. Figure 3a shows that the molecules returning to vacuum present a translational energy distribution characterized by a temperature well below T_s whether we consider all reflected molecules, only those that are reflected directly, or only those that come back to vacuum through a trapping−desorption mechanism. Figure 3b shows that no matter how long the molecules are trapped in the physisorption well, they will never fully thermalize in the physisorption well on Ir(111) at 1000 K. Trapped molecules with an absolute value of the translational momentum perpendicular to the surface ($p_{cm,z}$) larger than 20 au are not stable in the physisorption well and are absent from this distribution because they have enough kinetic energy perpendicular to the surface to escape toward vacuum and desorb. Figure 3c shows that molecules that remain trapped in the physisorption well for longer and longer times slowly approach a distribution of translational momentum parallel to the surface $p_{cm,x}$ (and also $p_{cm,y}$, not shown) corresponding to the surface temperature. However, it must be mentioned that the fraction of molecules that remain trapped in the physisorption well for ∼40 ps (the largest time considered in Figure 3b,c) represents a very small fraction of the initially trapped molecules because the great majority of them desorb at shorter times. Vibrational energy redistribution and quenching processes are typically even slower than those of translational degrees of freedom, which explains why in the low-energy precursor-mediated regime, S_0 strongly depends on the initial vibrational state of impinging molecules.[7] If the vibrations of trapped molecules rapidly thermalized on the surface, then S_0 would barely depend on the initial molecular vibrational state.

Interestingly, very small reactive sticking probabilities on flat metal surfaces are often attributed to reactive events taking place on the experimentally unavoidable surface defects (e.g., steps) that offer reaction pathways with energy barriers lower than those on terraces.[35,36] In particular, at low impact energies, the cross section of such more reactive sites increases because trapped molecules can more extensively explore the surface. Then, it might be argued that the low-energy mechanism observed experimentally might consist of molecular trapping followed by dissociation in steps. However, our calculations properly account for the contribution and the energy range where precursor-mediated dissociation is more relevant, without the need to include surface defects in the model. This points to the nonsignificant role of the steps in the experiments reported by the groups of Mullins[3] and Utz.[7]

Once we have shown that trapped molecules do not fully thermalize in a shallow physisorption well on a surface at 1000 K, it is clear that statistical concepts cannot be used to rationalize the T_s dependence of S_0 nor that of the α coefficient representing the probability of a trapped molecule to chemisorb. Still, the fraction of trapped molecules that finally chemisorb will depend on (nonthermal) temperature-dependent desorption and dissociation rates. We have found that larger surface temperatures favor desorption, and the mean lifetime of trapped molecules reduces from ∼20 ps at 800 K to ∼13 ps for 1000 K. Accordingly, the mean distance traveled by reactive molecules before dissociation also reduces, for example, from ∼90 Å for 800 K to ∼60 Å for 1000 K. To shed some light on the origin of the T_s dependence of S_{trapp} and S_{dir} and, in particular, their Arrhenius-like behavior (intriguingly with similar E_{app} values, as shown in Figure 2c), we have analyzed in detail the configurations for reactive molecules at the time that they dissociate directly and via the precursor-mediated mechanism. In line with the practically identical apparent activation energies, we have found no significant differences in the reactive geometries for these two mechanisms. In particular, we have found that in both cases, low-energy molecules only dissociate on top of an Ir atom that is instantaneously shifted up with respect to its nearest neighbors of the outermost surface layer. In Figure 4a, we represent the distribution of heights of reactive Ir atoms (at the dissociation time and relative to its six nearest neighbors in the surface plane), ΔZ_{Ir}, on which dissociation takes place for T_s = 1000 K and E_i = 0.01 eV. In this distribution, we consider both direct and precursor-mediated dissociation events. The blue vertical line indicates the optimum ΔZ_{Ir} value (i.e., ΔZ_{Ir}^{op} = 0.17 Å) obtained in a full geometry optimization of the lowest energy transition state for CH_4 dissociation on Ir(111).[35] It is observed that at low impact energies, most molecules dissociate on Ir atoms shifted up well above ΔZ_{Ir}^{op} for the minimum energy transition state. Such ΔZ_{Ir} displacements larger than ΔZ_{Ir}^{op} show that very low-energy molecules dissociate only through very low-energy barriers found for $\Delta Z_{Ir} \approx 0.4$ Å. (Here we talk about energy barriers without considering the energy cost of the lattice distortion that can be supplied by thermal fluctuations at high surface temperatures, E_b^*, in Figure 4b,) It is worth mentioning that a similar conclusion has recently been reached by Guo and Jackson for CH_4/Ni(211) at T_s = 500 K.[37] Thus a word of caution is needed here about the use of the energy of transition-state configurations obtained (as usual) through the full geometry optimization of both molecular and surface DOF without first checking if thermalization of the molecule−surface system is actually attained.

Interestingly, the distribution of heights of reactive Ir atoms is almost the same if we consider molecules that quickly dissociate through a direct mechanism or those that dissociate after having been trapped for a long time. The green and orange vertical lines in Figure 4a indicate the positions of the mean value of ΔZ_{Ir} ($<\Delta Z_{Ir}>$) for direct and precursor-mediated dissociation events, respectively, for T_s varying between 800 and 1000 K. The lowest $<\Delta Z_{Ir}>$ values are obtained for the lowest temperatures because the probability of a molecule encountering an Ir atom that is significantly shifted up is smaller. The fact that the $<\Delta Z_{Ir}>$ values for both direct and precursor-mediated dissociation mechanisms are similar indicates that at the high temperatures considered, Ir atoms are not much affected very much by the interaction with the molecules, even in the case of long interaction times. As previously mentioned, thermal fluctuations that create the lattice distortions give the molecules the possibility of encountering relatively low energy barriers for dissociation (see Figure 4b) with a probability that increases with surface temperature. For instance, a molecule that encounters an Ir

https://dx.doi.org/10.1021/acs.jpclett.0c00260
J. Phys. Chem. Lett. 2020, 11, 2211−2218

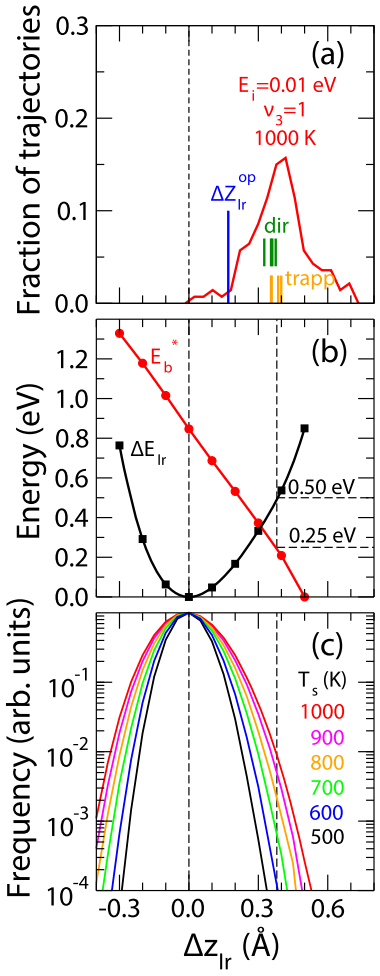

Figure 4. (a) Distribution of vertical displacements of the Ir atom, ΔZ_{Ir}, closest to $CH_4(\nu_3 = 1)$ when dissociation takes place for molecules with E_i = 0.01 eV and T_s = 1000 K. The green and orange vertical lines indicate the mean values of ΔZ_{Ir}, $<\Delta Z_{Ir}>$ obtained for direct and trapping-mediated dissociation events, respectively, for T_s = 700, 800, 900, and 1000 K. (b) Energy barrier for CH_4 dissociation on Ir(111) as a function of ΔZ_{Ir} for the Ir atom closest to the molecule (E_b^*, red line with symbols) the and energy cost of producing the displacement ΔZ_{Ir} (ΔE_{Ir}, black line with symbols). Note: The energy barrier, E_b, computed (as usual) including the energy cost of producing the lattice distortion is $E_b = E_b^* + \Delta E_{Ir}$. (c) Distribution of vertical displacements, ΔZ_{Ir}, of the outermost-layer Ir atoms of clean Ir(111) for different surface temperatures.

atom shifted up by $\Delta Z_{Ir} \approx 0.37$ Å (approximately the $<\Delta Z_{Ir}>$ value for T_s = 800−1000 K) must overcome an effective energy barrier, E_b^*, of only 0.25 eV, which is much more accessible for $CH_4(\nu_3 = 1)$ than for $CH_4(\nu = 0)$ because of its higher vibrational energy. The important point here is that such a lattice distortion that costs ∼0.5 eV is not frequent but occurs with some non-negligible probability at 1000 K due to thermal fluctuations. (See Figure 4c.)

The similarity between 0.53 eV (i.e., the E_{app} value obtained for both $S_{trapp}(T_s)$ and $S_{dir}(T_s)$ for E_i = 0.01 eV, Figure 2c) and the 0.5 eV necessary to produce an Ir displacement $\Delta Z_{Ir} = <\Delta Z_{Ir}>_{T_s=800-1000K}$ is not likely to be fortuitous. In fact, values of E_{app} similar to the energy cost of producing $\Delta Z_{Ir} = <\Delta Z_{Ir}>_{T_s=800-1000K}$ are also found for higher energy molecules. For instance, for $CH_4(\nu = 0)$ and E_i = 0.31, 0.41, and 1.11 eV, we have obtained $<\Delta Z_{Ir}> \approx 0.23$, 0.18, and 0.05 Å, for which ΔE_{Ir} is ∼0.21, 0.12, and 0.02 eV, respectively (see Figure 4b), all being close to the E_{app} values obtained in the QCT calculations for these impact energies (Figure 1b). Thus the apparent activation energy derived from the Arrhenius plots of both S_{trapp} and S_{dir} seems to be connected to the energy cost of producing the right lattice distortion required for the molecules to be able to dissociate either directly or after being trapped for a while. This is consistent with a picture of heavy Ir atoms moving almost independently of the interaction with the molecules whose temperature-dependent dissociation probability mostly depends on the typical instantaneous positions of the Ir atoms due to thermal fluctuation. Interestingly, using the sudden lattice model (SLM) widely employed to describe the T_s dependence of direct methane dissociation on transition-metal surfaces (see, e.g., ref 38 and references therein), we have found values of S_0 in good agreement with those shown in Figure 2a, even at low impact energies for which precursor-mediated dissociation is important. This is surprising a priori because precursor-mediated dissociation is certainly not a sudden process. (Its characteristic time is much longer than the typical period of lattice vibrations.) However, the weak dynamic coupling between molecular and lattice DOF in the precursor state allows S_{trapp} to be properly estimated while keeping the metal atoms fixed during the dynamics, as far as their positions are taken according to the thermal distribution of lattice distortions for the considered T_s value. Still, it is important to point out that the nonsudden character of the trapping process is put in evidence, for instance, by the too-large values of the precursor state lifetime obtained when using the SLM for T_s = 1000 K due to the lack of molecule−surface energy exchange.

In summary, we have performed molecular dynamics simulations to study the dissociative adsorption of CH_4 on Ir(111) as a function of impact energies and surface temperature, for molecules in the ground vibrational state and vibrationally excited state. Our QCT calculations give results that are in excellent agreement with experiments and allow us to shed new light on the way that precursor-mediated chemisorption takes place for CH_4/Ir(111) and its influence on the E_i and T_s dependence of S_0 at high surface temperatures close to those of real steam reforming catalysis. We have shown that dissociation proceeds through two distinct mechanisms depending on the impact energy of the molecules: precursor-mediated and direct. In contrast with the usual assumption about precursor-mediated chemisorption, both theory and experiments show that molecules do not thermalize in the physisorption well at the high temperatures for which catalytic steam reforming takes place in industry, that is, at ∼1000 K. Still, the weakly bound physisorbed state derived from the long-range molecule−surface interaction plays a crucial role in the low-energy precursor-mediated regime. It allows the molecules to become temporarily trapped, increasing the probability of finding active sites. However, in contrast with the usual belief, such active sites are not necessarily static defects (e.g., steps) but metal atoms instantaneously activated by the lattice distortions due to thermal fluctuations. The probability of a molecule finding such instantaneously active metal atoms sharply increases with surface temperature, and being induced by thermal fluctuations, this activates both direct and precursor-mediated mechanisms in a similar way. In the case of precursor-mediated dissociation, this thermal activation compensates for the reduced lifetime of the precursor state at high surfaces temperatures typical in

https://dx.doi.org/10.1021/acs.jpclett.0c00260
J. Phys. Chem. Lett. 2020, 11, 2211−2218

heterogeneous catalysis. To the best of our knowledge, this is the first time that such a theoretical description of precursor-mediated chemisorption dynamics of methane on metal surfaces from first-principles is reported in the literature. Our analysis introduces a fresh new way to think about and understand important underlying mechanisms happening in a catalyst during bond-breaking chemisorption.

■ ASSOCIATED CONTENT

Supporting Information

The Supporting Information is available free of charge at https://pubs.acs.org/doi/10.1021/acs.jpclett.0c00260.

Computational details. Figure S1: Optimized $V(\{\mathbf{r}\})$ (eqs 1−5) versus DFT energies for the configurations included in the database for fitting. RMSE obtained in the fitting of the DFT−PBE data with the potential $V(\{\mathbf{r}\})$ given in eqs 1−5 as a function of the maximum DFT energy considered, E_{max}. Table S1. RFF parameters defining $V(\{\mathbf{r}\})$ for CH_4/Ir(111). Table S2. Frequencies of CH_4 normal modes, ν_k, in cm^{-1} and their degeneracies, λ_k, obtained in DFT and RFF calculations and experimental data extracted from ref S20. Table S3: Comparison between the properties of the transition states obtained with DFT and the RFF. Figure S2: DFT and RFF values of E_b^* and ΔE_{Ir}. Probability of finding an outermost-layer Ir atom shifted in Z relative to the average Z position of its six nearest neighbors in the surface plane obtained in RFF-MD and AIMD calculations (PDF)

■ AUTHOR INFORMATION

Corresponding Authors

Wei Dong − *Université de Lyon, CNRS, Ecole Normale Supérieure de Lyon, Université Lyon 1, Laboratoire de Chimie, UMR 5182, 69364 Lyon, France; College of Chemistry and Chemical Engineering, Hunan University, 410082 Changsha, China;* orcid.org/0000-0003-3773-1029; Email: wei.dong@ens-lyon.fr

H. Fabio Busnengo − *Grupo de Fisicoquímica en Interfases y Nanoestructuras, Instituto de Física Rosario and Universidad Nacional de Rosario, 2000 Rosario, Argentina;* orcid.org/0000-0002-7532-8495; Phone: +54 (0)341-4853200/22; Email: busnengo@ifir-conicet.gov.ar

Authors

Raquel Moiraghi − *Instituto de Investigaciones en Fisicoquimica de Córdoba, CONICET, Universidad Nacional de Córdoba, X5000HUA Córdoba, Argentina*

Ariel Lozano − *Department of Electrical Engineering and Computer Science, University of Lige, B-4000 Lige, Belgium*

Eric Peterson − *Department of Chemistry and W. M. Keck Foundation Laboratory of Materials Science, Tufts University, Medford, Massachusetts 02155, United States*

Arthur Utz − *Department of Chemistry and W. M. Keck Foundation Laboratory of Materials Science, Tufts University, Medford, Massachusetts 02155, United States;* orcid.org/0000-0002-6525-594X

Complete contact information is available at: https://pubs.acs.org/10.1021/acs.jpclett.0c00260

Notes

The authors declare no competing financial interest.

■ ACKNOWLEDGMENTS

This work has been supported by ECOS-Sud (France) and MincyT (Argentina) through the bilateral project A11E06, MincyT (projects PICT Bicentenario N° 1962 and PICT 2016 N° 2750), CONICET (Argentina) (project PIP 0667), Universidad Nacional de Rosario (Argentina) (project PID ING235), China Hunan Provincial Science and Technology Department (project N° 2019RS1031, and the NSF (US) (project CHE-1800266). All the calculations have been performed in the HPC Cluster CCT-Rosario, member of SNCAD-Mincyt (Argentina).

■ REFERENCES

(1) Ertl, G. Reactions at Surfaces: From Atoms to Complexity (Nobel Lecture). *Angew. Chem., Int. Ed.* **2008**, *47*, 3524−3535.

(2) Larsen, J. H.; Chorkendorff, I. From fundamental studies of reactivity on single crystals to the design of catalysts. *Surf. Sci. Rep.* **1999**, *35*, 163−222.

(3) Seets, D. C.; Reeves, C. T.; Ferguson, B. A.; Wheeler, M. C.; Mullins, C. B. Dissociative chemisorption of methane on Ir(111): Evidence for direct and trapping-mediated mechanisms. *J. Chem. Phys.* **1997**, *107*, 10229−10241.

(4) Weaver, J. F.; Carlsson, A. F.; Madix, R. J. The adsorption and reaction of low molecular weight alkanes on metallic single crystal surfaces. *Surf. Sci. Rep.* **2003**, *50*, 107−199.

(5) Juurlink, L.; Killelea, D.; Utz, A. State-resolved probes of methane dissociation dynamics. *Prog. Surf. Sci.* **2009**, *84*, 69−134.

(6) Beck, R.; Utz, A. In *Dynamics of Gas-Surface Interactions*; Díez Muiño, R., Busnengo, H. F., Eds.; Springer Series in Surface Sciences *50*; Springer Berlin Heidelberg, 2013; Chapter 8, pp 179−212.

(7) Dombrowski, E.; Peterson, E.; Del Sesto, D.; Utz, A. Precursor-mediated reactivity of vibrationally hot molecules: Methane activation on Ir(111). *Catal. Today* **2015**, *244*, 10−18.

(8) Seets, D.; Wheeler, M.; Mullins, C. Mechanism of the dissociative chemisorption of methane over Ir(110): trapping-mediated or direct? *Chem. Phys. Lett.* **1997**, *266*, 431−436.

(9) Walker, A. V.; King, D. A. Dynamics of the Dissociative Adsorption of Methane on Pt110(1 × 2). *Phys. Rev. Lett.* **1999**, *82*, 5156−5159.

(10) Bisson, R.; Sacchi, M.; Beck, R. D. State-resolved reactivity of CH_4 on Pt(110)-(1 × 2): The role of surface orientation and impact site. *J. Chem. Phys.* **2010**, *132*, 094702.

(11) Kang, H. C.; Mullins, C. B.; Weinberg, W. H. Molecular adsorption of ethane on the Ir(110)(12) surface: Monte Carlo simulations and molecular beam reflectivity measurements. *J. Chem. Phys.* **1990**, *92*, 1397−1406.

(12) Busnengo, H. F.; Dong, W.; Salin, A. Trapping, Molecular Adsorption, and Precursors for Nonactivated Chemisorption. *Phys. Rev. Lett.* **2004**, *93*, 236103.

(13) Beutl, M.; Riedler, M.; Rendulic, K. D. Strong rotational effects in the adsorption dynamics of H_2/Pd(111): evidence for dynamical steering. *Chem. Phys. Lett.* **1995**, *247*, 249−252.

(14) Steinrück, H. P.; Luger, M.; Winkler, A.; Rendulic, K. D. Adsorption probabilities of H_2 and D_2 on various flat and stepped nickel surfaces. *Phys. Rev. B: Condens. Matter Mater. Phys.* **1985**, *32*, 5032−5037.

(15) Berger, H.; Resch, C.; Grösslinger, E.; Eilmsteiner, G.; Winkler, A.; Rendulic, K. Adsorption of hydrogen on tungsten: a precursor path plus direct adsorption. *Surf. Sci.* **1992**, *275*, L627−L630.

(16) Gee, A. T.; Hayden, B. E.; Mormiche, C.; Nunney, T. S. The role of steps in the dynamics of hydrogen dissociation on Pt(533). *J. Chem. Phys.* **2000**, *112*, 7660−7668.

(17) Rettner, C. T.; Stein, H.; Schweizer, E. K. Effect of collision energy and incidence angle on the precursormediated dissociative chemisorption of N_2 on W(100). *J. Chem. Phys.* **1988**, *89*, 3337−3341.

(18) Rettner, C. T.; Schweizer, E. K.; Stein, H. Dynamics of the chemisorption of N_2 on W(100): Precursormediated and activated dissociation. *J. Chem. Phys.* **1990**, *93*, 1442−1454.
(19) Beutl, M.; Rendulic, K.; Castro, G. Does the rotational state of a molecule influence trapping in a precursor? An investigation of N_2/W(100), CO/FeSi(100) and O_2/Ni(111). *Surf. Sci.* **1997**, *385*, 97−106.
(20) Luntz, A. C.; Williams, M. D.; Bethune, D. S. The sticking of O_2 on a Pt(111) surface. *J. Chem. Phys.* **1988**, *89*, 4381−4395.
(21) Mullins, C. B.; Weinberg, W. H. Trapping-mediated dissociative chemisorption of ethane on Ir(110)(1 × 2). *J. Chem. Phys.* **1990**, *92*, 4508−4512.
(22) Bowker, M. The Role of Precursor States in Adsorption, Surface Reactions and Catalysis. *Top. Catal.* **2016**, *59*, 663−670.
(23) Sitz, G. O.; Mullins, C. B. Molecular Dynamics Simulations of the Influence of Surface Temperature On the Trapping of Methane on Iridium Single-Crystalline Surfaces. *J. Phys. Chem. B* **2002**, *106*, 8349−8353.
(24) Killelea, D. R.; Utz, A. L. On the origin of mode- and bond-selectivity in vibrationally mediated reactions on surfaces. *Phys. Chem. Chem. Phys.* **2013**, *15*, 20545−20554.
(25) Shirhatti, P. R.; Rahinov, I.; Golibrzuch, K.; Werdecker, J.; Geweke, J.; Altschäffel, J.; Kumar, S.; Auerbach, D. J.; Bartels, C.; Wodtke, A. M. Observation of the adsorption and desorption of vibrationally excited molecules on a metal surface. *Nat. Chem.* **2018**, *10*, 592−598.
(26) Utz, A. L. Vibrations that live long and prosper. *Nat. Chem.* **2018**, *10*, 577−578.
(27) Huang, M.; Zhou, X.; Zhang, Y.; Zhou, L.; Alducin, M.; Jiang, B.; Guo, H. Adiabatic and nonadiabatic energy dissipation during scattering of vibrationally excited CO from Au(111). *Phys. Rev. B: Condens. Matter Mater. Phys.* **2019**, *100*, 201407.
(28) Nattino, F.; Ueta, H.; Chadwick, H.; van Reijzen, M. E.; Beck, R. D.; Jackson, B.; van Hemert, M. C.; Kroes, G.-J. Ab Initio Molecular Dynamics Calculations versus Quantum-State-Resolved Experiments on CHD_3 + Pt(111): New Insights into a Prototypical Gas-Surface Reaction. *J. Phys. Chem. Lett.* **2014**, *5*, 1294−1299.
(29) Tersoff, J. New empirical approach for the structure and energy of covalent systems. *Phys. Rev. B: Condens. Matter Mater. Phys.* **1988**, *37*, 6991−7000.
(30) Xiao, Y.; Dong, W.; Busnengo, H. F. Reactive force fields for surface chemical reactions: A case study with hydrogen dissociation on Pd surfaces. *J. Chem. Phys.* **2010**, *132*, 014704.
(31) Shen, X. J.; Lozano, A.; Dong, W.; Busnengo, H. F.; Yan, X. H. Towards Bond Selective Chemistry from First Principles: Methane on Metal Surfaces. *Phys. Rev. Lett.* **2014**, *112*, 046101.
(32) Perdew, J. P.; Burke, K.; Ernzerhof, M. Generalized Gradient Approximation Made Simple. *Phys. Rev. Lett.* **1996**, *77*, 3865−3868.
(33) Lozano, A.; Shen, X.; Moiraghi, R.; Dong, W.; Busnengo, H. Cutting a chemical bond with demon's scissors: Mode- and bond-selective reactivity of methane on metal surfaces. *Surf. Sci.* **2015**, *640*, 25−35.
(34) Chen, L.; Ueta, H.; Chadwick, H.; Beck, R. D. The Negligible Role of C−H Stretch Excitation in the Physisorption of CH_4 on Pt(111). *J. Phys. Chem. C* **2015**, *119*, 14499−14505.
(35) Moiraghi, R.; Lozano, A.; Busnengo, H. F. Theoretical Study of the Dissociative Adsorption of Methane on Ir(111): The Role of Steps and Surface Distortions at High Temperatures. *J. Phys. Chem. C* **2016**, *120*, 3946−3954.
(36) Zhou, X.; Jiang, B.; Guo, H. Dissociative Chemisorption of Methane on Stepped Ir(332) Surface: Density Functional Theory and Ab Initio Molecular Dynamics Studies. *J. Phys. Chem. C* **2019**, *123*, 20893−20902.
(37) Guo, H.; Jackson, B. Methane dissociation on stepped Ni surfaces resolved by impact site, collision energy, vibrational state, and lattice distortion. *J. Chem. Phys.* **2019**, *150*, 204703.
(38) Jackson, B. In *Dynamics of Gas-Surface Interactions*; Díez Muiño, R., Busnengo, H. F., Eds.; Springer Series in Surface Sciences *50*; Springer Berlin Heidelberg, 2013; Chapter 9, pp 213−237.

https://dx.doi.org/10.1021/acs.jpclett.0c00260
J. Phys. Chem. Lett. 2020, 11, 2211−2218